DOI: 10.1002/ejic.201000080

Studies on the Formation of CdS Nanoparticles from Solutions of $(NMe_4)_4[Cd_{10}S_4(SPh)_{16}]$

Maria Bendova,[a] Michael Puchberger,[a] Silvia Pabisch,[b] Herwig Peterlik,[b] and Ulrich Schubert*[a]

Keywords: Cadmium / Cadmium sulfide / Nanoparticles / Cluster compounds / S ligands / Rearrangement

The stepwise cluster growth, and formation of CdS nanoparticles from solutions of $(NMe_4)_4[Cd_{10}S_4(SPh)_{16}]$ in dimethyl sulfoxide (DMSO), dimethylformamide (DMF) and acetonitrile was investigated. Cluster growth is fast in DMSO and DMF at room temperature, and slow in acetonitrile at elevated temperatures. Larger sulfide clusters (initially Cd_{32}, then Cd_{54}) are initially formed, which upon further growth eventually give rise to CdS nanoparticles. Strong evidence was found that the byproduct formed during the reaction in DMSO is mononuclear $[Cd(SPh)_x(DMSO)_y]^{(2-x)}$ ($x \approx 3$).

Introduction

Semiconductor nanoparticles (NPs) or nanocrystals have drawn much attention in fundamental research and material applications due to their size-dependent properties.[1,2] There is a clear correlation between the NP size and its excitonic transition energy due to quantum size effects. The absorption shifts to higher wavelengths with increasing size, until the characteristics of a bulk CdS are reached at a diameter of about 6 nm.[1–4] Clusters are of particular interest as molecular models for semiconductor NPs, because they have a defined molecular structure and thus unequivocal UV/Vis characteristics. The absorption maxima of the clusters are clearly size-dependent. For example, the maxima of Cd_{17}, Cd_{32} and Cd_{54} sulfide clusters are around 290, 325 and 350 nm, respectively.[4–7]

A series of molecular, thiolate-capped cadmium sulfide clusters of different size were structurally characterized in the solid state, ranging from $[Cd_{10}S_4(SPh)_{16}]^{4-}$ (**1**),[8] $[Cd_{17}S_4(SPh)_{28}]^{2-}$ [9]/$Cd_{17}S_4(SCH_2CH_2OH)_{26}$ [5] (Cd_{17}) and $Cd_{32}S_{14}(SR)_{36}L_4$ [10,11,6]/$[Cd_{32}S_{14}(SPh)_{40}]^{4-}$ [4,12] (Cd_{32}) to $[Cd_{54}S_{32}(SPh)_{48}L_4]^{4-}$ [4]/$Cd_{54}S_{28}(SPh)_{52}L_4$ [7] (Cd_{54}). However, their molecular structures in solution are not necessarily the same as that in the solid state. Solvents influence very much their stability in solution and can cause exchange of stabilizing ligands and/or rearrangement processes.

One of the best methods for investigation of the solution behavior of CdS or CdSe clusters is ^{113}Cd NMR, and for CdSe clusters also ^{77}Se NMR spectroscopy. The results have been reviewed previously.[13] NMR investigation of the $Cd^{2+}/S^{2-}/SPh^-$/dimethylformamide (DMF) system revealed that Cd_8 (e.g. $[Cd_8S(SPh)_{16}]^{2-}$ [14]), Cd_{10} (**1**) and Cd_{17} clusters ($[Cd_{17}S_4(SPh)_{28}]^{2-}$) are in dynamic equilibrium, depending on the concentration and cluster composition. It was concluded that the thermodynamic stability of the clusters decreases in the order $Cd_8 > Cd_{10} > Cd_{17}$, and solubility of their NMe_4^+ salts increases in the order $Cd_{10} < Cd_{17} < Cd_8$. As a consequence, Cd_8 clusters are formed in DMF solutions of Cd_{10} or Cd_{17} clusters at room temperature (high stability of Cd_8 cluster). If the solution contains only Cd_8 and Cd_{17} clusters, addition of NMe_4Cl causes their conversion to the Cd_{10} cluster which crystallizes from this solution as the NMe_4^+ salt of Cd_{10} is the least soluble species. Electrospray mass spectrometry investigations on **1** in acetonitrile solution revealed its tendency to lose $[Cd(SPh)_3]^-$ and SPh^- species.[15]

Exchange reactions in DMF solutions were also investigated.[16] With increasing CdS cluster size (e.g. from Cd_4 to Cd_{10}) the exchange reactions become substantially slower at room temperature. Mixing of $[Cd_{10}S_4(SPh)_{16}]^{4-}$ and $[Zn_{10}S_4(SPh)_{16}]^{4-}$ in DMF showed that exchange of the outer metal atoms (M^o) is complete within minutes and that M^o prefer a core of the same metal. Exchange of the inner metal atoms (M^i) takes hours at room temperature, resulting in scrambling of M^i. Mixing of $[Cd_{10}S_4(SPh)_{16}]^{4-}$ and $[Cd_{10}Se_4(SPh)_{16}]^{4-}$ in DMF showed that 50% of the μ_3-S atoms were exchanged in about 4 d at room temperature. Exchange rates are inversely related to the distance from the surface of the molecule.

Most of these investigations were performed in DMF because of the high solubility of the clusters, which is necessary for obtaining high-quality ^{113}Cd NMR spectra, and because it allows cooling to –60 °C to slow down exchange reactions. On the other hand, DMF is a coordinating solvent and can lead to cluster degradation in solution.

[a] Institute of Materials Chemistry, Vienna University of Technology,
Getreidemarkt 9, 1060 Wien, Austria
[b] Faculty of Physics, University of Vienna,
Boltzmanngasse 5, 1090 Wien, Austria

Supporting information for this article is available on the WWW under http://dx.doi.org/10.1002/ejic.201000080.

WILEY InterScience DISCOVER SOMETHING GREAT
© 2010 Wiley-VCH Verlag GmbH & Co. KGaA, Weinheim

Several researchers observed rearrangement of smaller CdS/CdSe clusters in strongly coordinating solvents and formation of larger CdS/CdSe NPs. Herron et al.[10] obtained a Cd_{32} cluster from a pyridine solution of $Cd_{10}S_4(SPh)_{12}$ after addition of DMF. They proposed that pyridine causes rapid fracture of the cluster core into a mixture of species with lower nuclearities which assemble and form larger species. The latter are in fast exchange with smaller species. A Cd_{32} cluster crystallized from the system as the least soluble species. Strouse et al. investigated the formation of semiconductor NPs from M_{10} (CdS/CdSe/ZnS/ZnSe) clusters, being similar to **1**, in hexadecylamine (HDA). Formation of 2–9 nm HDA-stabilized CdSe NPs was observed after slow heating of $Li_4[Cd_{10}Se_4(SPh)_{16}]$ in HDA to 220–240 °C.[17] It was proposed that the mechanism of NP formation is a combination of ligand exchange reactions and fragmentation related to the loss of apical $[Cd(SePh)_3]^-$ species from the precursor cluster followed by aggregation of Cd_xSe_y species. However, the authors were not able to characterize any byproducts that would have supported their mechanistic proposal. Further investigations on transformations of clusters similar to **1** in HDA at elevated temperatures were subsequently carried out.[18–22] DeGroot et al.[19] reacted the mixed-metal cluster $M_{10}Se_4(SePh)_{12}(PPr_3)_4$ (M = Cd+Zn) in HDA at 120–240 °C. Zn atoms preferably occupy apex M° positions in the M_{10} clusters, according to NMR studies in CD_2Cl_2 and crystal structure analyses.[23] The formed NPs revealed the same Cd:Zn ratio as the precursor which implies that release of the M° positions is not preferred. This conclusion should be applicable also to the mono-metallic Cd_{10} cluster, but is in disagreement with the mechanism proposed by Cumberland et al.[17] However, the molecular structures and exchange dynamics of M_{10} clusters used in the study of DeGroot et al.[19] could be different in HDA reaction solutions[19] than in CD_2Cl_2 solutions,[23] and, also, charge differences between the neutral[19] and negatively charged Cd_{10} clusters[17] can have an influence. Furthermore, the formation of diphenyl diselenide Ph_2Se_2 at 120–160 °C was confirmed by GC/MS analyses.[19] Its proportion decreased with increasing reaction temperature, concurrent with the appearance of diphenyl selenide Ph_2Se. The authors considered the presence of Ph_2Se_2 in the GC/MS spectra as an indication of the presence of $[M(SePh)_2]$ or $[M(SePh)_3]^-$ species.[19] Finally, Lovingood et al.[20] proved the formation of CdSSe NPs instead of CdSe NPs[17] from $Li_4[Cd_{10}Se_4(SPh)_{16}]$ in HDA. NPs prepared at higher temperatures (230 °C) had a higher S^{2-} proportion compared to those prepared at 120 °C. S^{2-} originates from the decomposition of PhS^- at higher temperatures to give Ph_2S and S^{2-}. The overall decomposition reaction can be formally written as Equation (1).

$$Li_4[Cd_{10}Se_4(SPh)_{16}] \longrightarrow (Cd_{10}Se_4S_6) + 6\ Ph_2S + 4\ LiSPh \quad (1)$$

In this paper we will prove that the cluster core of $[Cd_{10}S_4(SPh)_{16}]^{4-}$ (**1**) in DMSO solutions first grows to give larger clusters before CdS NPs are formed. In previous reports on the growth of **1** and similar clusters and on the formation of CdS NPs in hexadecylamine (HDA)[17,21] the mechanism was not satisfactorily clarified. To this end, we tried to identify the byproducts formed during the cluster growth. We will show that $[Cd(SPh)_x(DMSO)_y]^{(2-x)}$ ($x \approx 3$) species are involved in agreement with the predictions of Cumberland et al.[17]

Results and Discussion

Two different crystal structures of $(NMe_4)_4[Cd_{10}S_4(SPh)_{16}]$ (**1**) were previously obtained. The first, space group $I\bar{4}$, was obtained by adding water to a hot DMF solution and the second (space group $I\bar{4}2m$ or $P\bar{4}2_1c$) by cooling a hot saturated acetonitrile solution.[8] We were able to crystallize the cluster in a third modification (**1a**, space group *Aba*2, Figure 1) by adding toluene to a DMSO solution of **1**. The structures differ only in the orientation of PhS ligands.

The UV/Vis spectra of acetonitrile, DMSO and DMF solutions of **1** as well as dynamic light scattering (DLS) measurements (Figure 2) showed substantial differences. In acetonitrile, the absorption maxima were at 290, 256 and 207 nm, which is in good agreement with previous reports.[24] The hydrodynamic radius is <1.5 nm with a maximum at 0.5 nm. Similar data were obtained for DMF solution, viz. a shoulder at ca. 310 nm and a hydrodynamic radius < 2 nm with a maximum at 0.5 nm. In contrast, the absorption maximum in DMSO was at 336 nm, and the hydrodynamic radius was < 3 nm with a maximum at 0.8 nm. These observations were a first indication that **1** grows or agglomerates/aggregates in DMSO solution.

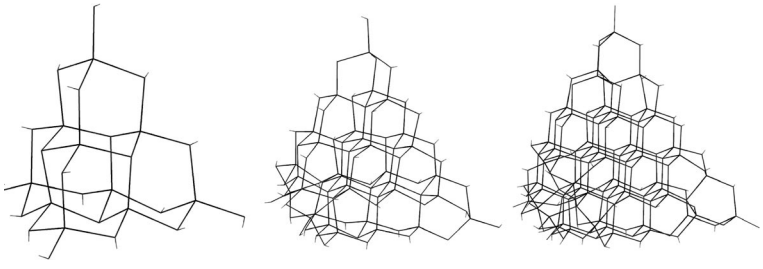

Figure 1. Line drawings of the clusters $[Cd_{10}S_4(SPh)_{16}]^{4-}$ (in **1a**) (left), $[Cd_{32}S_{14}(SPh)_{40}]^{4-}$ (center), and $[Cd_{54}S_{32}(SPh)_{48}L_4]^{4-}$ (right).

 © 2010 Wiley-VCH Verlag GmbH & Co. KGaA, Weinheim

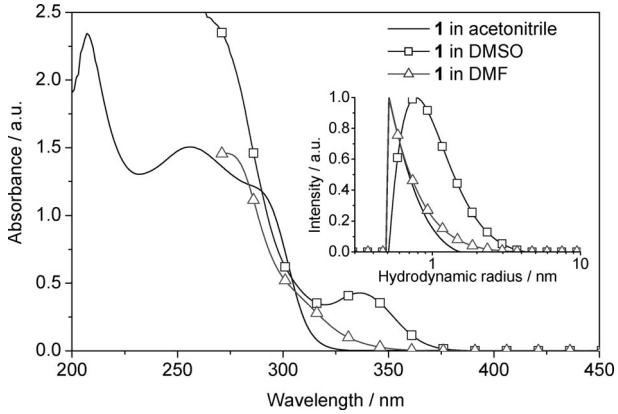

Figure 2. UV/Vis spectra of **1** in different solvents (0.02 mg/mL in acetonitrile, 0.08 mg/mL in DMSO, 0.025 mg/mL in DMF). Insert: DLS hydrodynamic radii distribution functions of **1**.

NMR measurements of **1** in [D_3]acetonitrile, [D_6]DMSO and [D_7]DMF solutions showed also substantial differences (Figure S1). Two PhS groups with an intensity ratio of 3:1 were observed in the ^{1}H NMR spectrum in [D_3]acetonitrile solution. The two sets of resonances were assigned to bridging [7.54 (d, 2 H), 6.88 (m, 3 H) ppm] and terminal groups [7.19 (d, 2 H), 6.79 (m, 3 H) ppm]. The terminal group showed ^{1}H-^{113}Cd correlation to one Cd signal (outer Cd, labeled Cd^o, at δ = 602 ppm), the bridging group to both Cd signals (Cd^o and inner Cd, labeled Cd^i, at δ = 687 ppm). The NMR spectroscopic data are in agreement with the solid-state structures of **1** (Figure 1).[8,16]

In contrast, *three* sets of PhS NMR signals were observed for [D_6]DMSO solutions. Two of them correlate to Cd signals (598.5, 680 ppm) in the ^{1}H-^{113}Cd HMBC spectra similar to the acetonitrile solution. They were therefore assigned to bridging [7.43 (d, 2 H), 6.76 (m, 3 H) ppm] and terminal [7.13 (d, 2 H), 6.73 (m, 3 H) ppm] groups. The third group [7.32 (d, 2 H), 6.89 (t, 2 H), 6.76 (m overlapped, 1 H) ppm] did not show a correlation to Cd and was thus assigned to an "unknown" PhS group. The chemical species giving rise to this signal is one of the main issues in the remainder of this article. Interestingly, the ratio of the PhS peak intensities changed with time; the proportion of the "unknown" PhS group increased and that of bridging and terminal decreased, but the ratio between bridging and terminal remained 3:1. Furthermore, a second [D_6]DMSO solvent signal (2.525 ppm) was observed, due to coordinated solvent.

Similar, but less pronounced, observations were made for a [D_7]DMF solution of **1**. Three PhS groups in the ^{1}H NMR spectrum were again assigned to bridging [7.67 (d, 2 H), 6.76 (m, 3 H) ppm], terminal [7.26 (d, 2 H), 6.76 (m, 2 H), 6.66 (m, 1 H) ppm] and "unknown" [7.48 (d, 2 H), 6.90 (m overlapped, 2 H), 6.77 (m overlapped, 1 H) ppm] PhS groups. The ratio of the bridging and terminal PhS groups was around 3:1 and remained approximately constant with time. The intensity of the "unknown" PhS group increased with time, but slower than in [D_6]DMSO solution. In the ^{113}Cd NMR spectrum, two signals were obtained (598 and 682.5 ppm) which were very similar to that in [D_3]acetonitrile and [D_6]DMSO solutions.

NMR investigation of **1** in [D_7]DMF was previously performed by Dance et al.[25] They focused on ^{113}Cd and ^{13}C NMR spectra, which revealed the presence of two sets of PhS ligands, bridging and terminal. They coalesced at ca. 340 K due to intramolecular exchange as proposed by Hagen et al. for $[Cd_4(SPh)_{10}]^{2-}$.[26] No other PhS groups were mentioned. Lee et al.[9] recorded time and temperature-dependent ^{113}Cd NMR spectra of DMF solutions of $(NMe_4)_2[Cd_{17}S_4(SPh)_{28}]$ and postulated fast and slow rearrangement processes. This could be similar with the observed NMR behavior of **1** in DMF and DMSO solutions.

However, this cannot explain the growth of the cluster core of **1** in DMSO, which was indicated by UV/Vis and DLS measurements. The assumption that DMSO and/or DMF could cause cluster agglomeration is not very likely, because this kind of behavior is not typical for strongly coordinating solvents. The influence of semiconductor particle-particle interactions on their spectroscopic behavior was investigated by several groups. Vossmeyer et al.[27] observed that the absorption maxima of small, almost monodisperse 1-thioglycerol-stabilized CdS NPs shifted to higher wavelengths (from 260 to 270 nm) when closely packed in layers. The shift was most pronounced for the smallest NPs with 0.64 nm radius, which corresponds to clusters of approximately ten Cd atoms. This was explained by collective electronic modes similar to the energy bands of conventional bulk semiconductors. Döllefeld et al.[28] investigated the absorption of solid nanocrystal assemblies of defined Cd_{17} clusters stabilized by 2-mercaptoethanol and observed a shift of absorption in solution and in solid state from 290 to 305 nm. They explained this observation by calculations involving electronic and dipole-dipole interactions and found that the shift was higher for smaller NPs with smaller mutual distances. In both cases[27,28] a red shift of about 10–15 nm was reported for semiconductor NP arrays compared with separated NPs. We observed a red shift of ca. 50 nm for **1** in DMSO compared with acetonitrile solution. This shift is too high to be explained by only cluster agglomeration.

To find an explanation for the observed UV/Vis, DLS and NMR spectroscopic data of **1** in DMSO solution, we investigated DMSO solutions in two series of experiments, viz. time-dependence at room temperature (series A), and time-dependence at 80 °C (series B).

Series A. A solution of 10 mg/mL of **1** in DMSO was stored at room temperature. DLS data (Figure 3, insert) indicated continuous growth of the cluster. However, the UV/Vis absorptions (Figure 3) were not typical for continuously growing NPs. After about one week, two distinct maxima at ca. 348 and ca. 325 nm were dominant in the spectra (their positions did not change with time). The ratio between the maxima at 348 to 325 nm was slightly increasing with time. According to other investigations,[7] these spectroscopic features are tentatively assigned to two clusters with distinct molecular structures, viz. $[Cd_{54}S_{32}(SPh)_{48}$-

 © 2010 Wiley-VCH Verlag GmbH & Co. KGaA, Weinheim

$(DMSO)_4]^{4-}$ and $Cd_{32}S_{14}(SPh)_{36}(DMSO)_4$ (similar to other Cd_{54} and Cd_{32} clusters with other neutral ligands). Thus, the Cd_{54}/Cd_{32} cluster ratio is increasing with time.

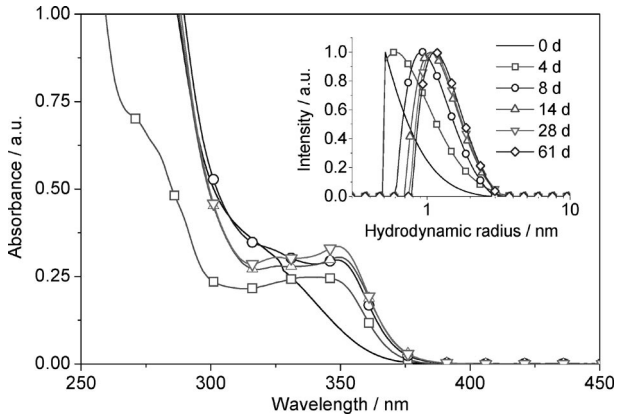

Figure 3. UV/Vis spectra of **1** in DMSO after different time periods (up to 61 d) at room temperature. Solutions were diluted for measurements to concentration 0.07 mg/mL. Insert: Corresponding DLS hydrodynamic radii distribution functions.

The "unknown" PhS group was again observed in ^{1}H NMR investigations (10 mg/mL in [D_6]DMSO), and its intensity increased with time as described above. After 19 d, only the "unknown" PhS group was present, together with ca. 5% of diphenyl disulfide [7.53 (d, 2 H), 7.38 (t, 2 H), 7.28 (t, 1 H) ppm]. Chemical shifts of the "unknown" PhS group changed slightly with time. A similar NMR experiment was also performed with a [D_7]DMF solution of **1** (10 mg/mL). After 27 d at room temperature, ca. 45% of all PhS groups belonged to cluster **1**, the rest to the "unknown" group.

Series B. Solutions of **1** in DMSO with different cluster concentrations (10 or 40 mg/mL) were heated at 80 °C for 16 or 72 h (samples B1–B4, see Table 1). DLS hydrodynamic radii distributions were similar for all samples, but differed to that of the experiments in Series A. While the radius was between 0.8 and 3.5 nm for the sample in Series A after 61 d (Figure 3), the radii in Series B were larger (1–5 nm). The UV/Vis data are summarized in Table 1. In addition to the absorption maxima, we also used the first derivatives of the absorption curves for the evaluation of the spectra, which facilitates distinction of CdS clusters or NPs of different sizes (see Figure 4 as an example, for more details see Figure S2). We define an absorption edge as an inflection point of the absorption curve, i.e. a minimum of the first derivative curve.[29] Table 1 contains two different values for absorption edge/maximum, those of the more pronounced excitonic transition of smaller NPs and, in parentheses, that of the less pronounced excitonic transition of larger NPs, which is expressed by a shoulder (samples B1, B2) or a smaller maximum (samples B3, B4). Samples B1 and B2 showed an additional small shoulder at ca. 325 nm (not listed in Table 1).

Table 1. Summary of UV/Vis data for **1** in DMSO after heating at 80 °C.

Sample	Sample conc. [mg/mL]	Heating time [h]	Conc. for UV/Vis [mg/mL]	Absorption edge/ maximum [nm]
B1	10	16	0.11	(ca. 380/?) 366/348
B2	40	16	0.13	(386/ca. 380) 361/346
B3	10	72	0.15	(396/ca. 376) 365/ca. 348
B4	40	72	0.13	(396/ca. 375) 354/ca. 340

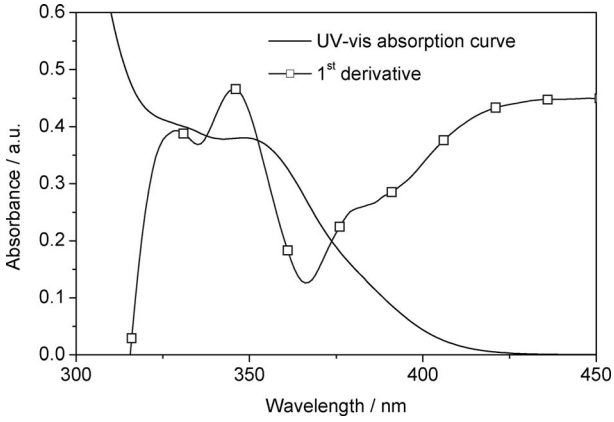

Figure 4. Analysis of UV/Vis data for sample B1. The shoulder at ca. 380 nm is not clearly visible in the spectrum, only in the first derivative.

In summary, samples heated for 16 h (B1 and B2) contain Cd_{32}, Cd_{54} and larger clusters with an absorption edge at ca. 380–385 nm. Samples heated for 72 h (B3 and B4) contain Cd_{54} (B4 only probably) and larger clusters with an absorption edge at 396 nm and maximum at ca. 375 nm.

We also investigated the development of the UV/Vis spectra of the DMSO solutions of **1** (10 mg/mL) during heat treatment in regular intervals (Figure 5). Formation of Cd_{54} clusters was the main feature during the first 4 h of heat treatment. Then the formation of larger NPs was noticed with absorption edges starting at ca. 380 and ending at ca. 410 nm after 330 h. This corresponds to NP diameters of about 2.1 and 3.0 nm, respectively.[30] The band characteristics for the Cd_{54} cluster disappeared concomitantly and new features appeared. The UV/Vis spectra indicated that the size distribution of the biggest NPs was broader with increasing heating periods. The results were similar for a cluster concentration of 40 mg/mL although NPs larger than Cd_{54} were formed earlier than in the 10 mg/mL sample (see Figure S3).

^{1}H NMR spectra of a 10 mg/mL sample showed the same behavior as in Series A. Signals for **1** disappeared faster, and after 90 min at 80 °C only the "unknown" SPh group was present. The spectra did not change during 4 d of heating at 80 °C. Formation of ca. 5% of diphenyl disulfide was again observed. We did not obtain signals in the ^{113}Cd NMR spectrum. ^{1}H NMR spectra of the B2 sample (40 mg/mL, 80 °C/16 h) revealed the presence of the same "unknown" PhS group. The chemical shifts for the aromatic *meta* and *para* protons differed slightly (± 0.2 ppm), but the

 © 2010 Wiley-VCH Verlag GmbH & Co. KGaA, Weinheim

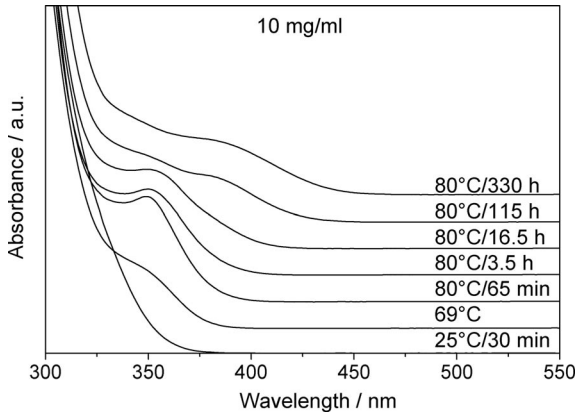

Figure 5. UV/Vis absorption spectra of **1** in DMSO (10 mg/mL) after different heating periods.

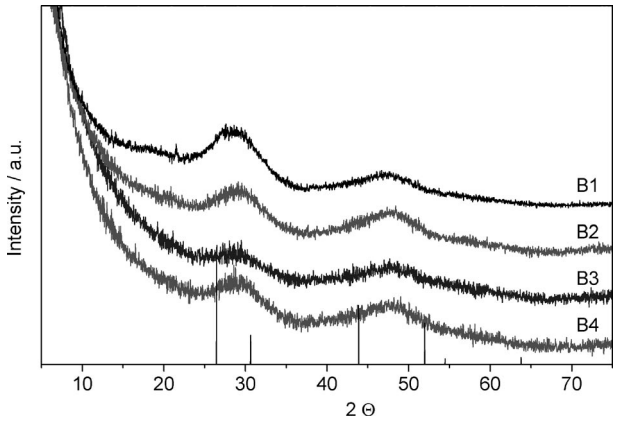

Figure 6. X-ray powder diffractogram of CdS NPs isolated from samples B1–B4 by addition of toluene. Bars represent sphalerite CdS.

^{13}C chemical shifts were almost the same. We obtained three broad, weak signals in the ^{113}Cd NMR spectrum at 593, 517 and 67 ppm (Figure 8), which will be discussed later.

DMF and acetonitrile solutions of **1** (10 mg/mL, 16 h) were heated to 80 and 75 °C, respectively. Changes were monitored by NMR and UV/Vis absorption and were similar to the DMSO solution. Absorption maxima of the biggest NPs were at 369 and 354 nm in DMF and acetonitrile. However, according to NMR and absorption spectra, the acetonitrile solution still contained an appreciable proportion of the cluster **1** (ca. 75%) after 16 h of heating.

The CdS NPs prepared in samples B1–B4 were precipitated from the reaction solutions by addition of a >3-fold excess of toluene. The precipitate was separated by sedimentation or centrifugation, washed with toluene and dried in vacuo. The solid yield was ca. 45 wt.-% for samples B1 and B2, and ca. 25 wt.-% for B3 and B4 samples, relative to **1**. Powder XRD measurements of the precipitates confirmed the presence of very small CdS NPs (Figure 6). The modification (wurtzite or sphalerite) could not be identified precisely because of the small particle size. Since the size of very small NPs cannot be calculated with sufficient accuracy from Scherrer's equation we also performed SAXS investigations. Scattering curves for samples B1–B4 are shown in Figure 7.

The scattering intensities $I(q)$ were fitted with asymmetric Gaussian and Lorentzian functions for the samples with lower and higher concentration, respectively. The peak maxima and half-widths were converted to distances and distribution widths in real space. They are attributed to a short range order of NPs, which gives the size of the NPs in the case of hard spheres arranged close to each other. The data are summarized in Table 2. There is an obvious asymmetry towards smaller sizes in real space (i.e. towards larger q-values in reciprocal space as seen in Figure 7). This supports the notion that the average size of the particles increases continuously. The growth is controlled by the sample concentration as well as by time: The particle distance, and therefore the size as well, grows from 2.13 nm and 2.86 nm after 16 h (B1 and B2) to 2.37 nm and 3.51 nm

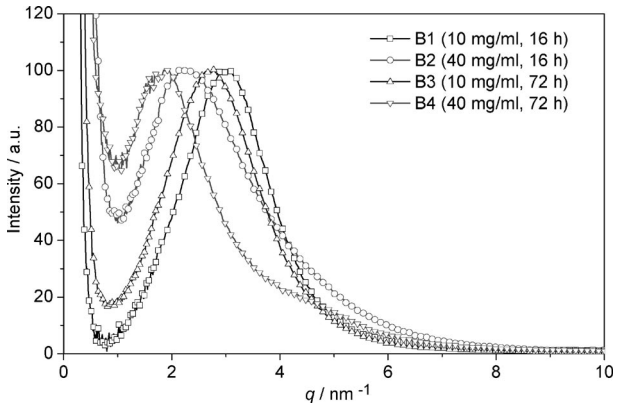

Figure 7. SAXS scattering curves of CdS NPs isolated from samples B1–B4 by addition of toluene. The curves were normalized for the same height of the scattering peak.

after 72 h (B3 and B4). The distance distribution is significantly more asymmetric in the case of the higher concentrations (B2 and B4) as in the lower ones (B1 and B3). This leads to the conclusion that there is a more uniform growth in the latter case. In sample B4, a very weak peak at about q = 4.7 nm^{-1} was observed, which corresponds to a distance of 1.3 nm in real space. A cluster-cluster aggregation, however, is quite improbable, as there is no significant scattering intensity towards high q-values.

Table 2. NP–NP distance and half-width from the asymmetric fits for the CdS NPs isolated from samples B1–B4 by addition of toluene.

Sample	NP distance [nm]	Asymmetric half-widths [nm]
B1	2.13	+ 0.50/–0.79
B2	2.86	+ 1.2/–2.4
B3	2.37	+ 0.64/–1.0
B4	3.51	+ 1.4/–2.8

CdS NPs obtained from sample B2 by precipitation with toluene were further characterized by solid-state ^{13}C and ^{113}Cd NMR spectroscopy. ^{13}C NMR spectra showed the presence of PhS^- and Me_4N^+ groups. ^{113}Cd NMR showed only very weakly resolved broad signals at ca. 600, ca. 680

 © 2010 Wiley-VCH Verlag GmbH & Co. KGaA, Weinheim

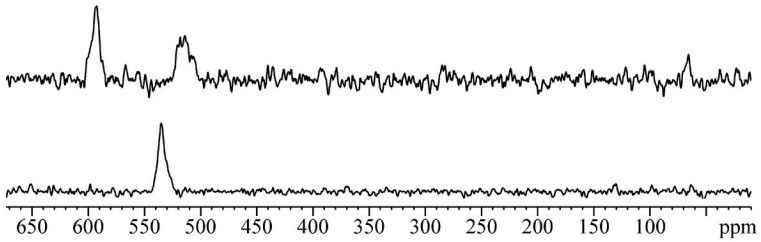

Figure 8. ^{113}Cd NMR spectrum of B2 sample in [D_6]DMSO (40 mg/mL, 80 °C/16 h) before (top) and after (bottom) 1:1 molar addition of $(NMe_4)_2[Cd(SPh)_4]$ (**2**).

and ca. 730 ppm. Since we assume formation of PhS-capped CdS NPs in the DMSO solutions, these results can be compared with solid-state ^{113}Cd NMR spectra of sphalerite PhS-capped CdS NPs of various sizes measured by Herron et al.[31] Sharp resonances at δ = 586 ppm were assigned to Cd only coordinated by PhS {as it was also observed for $[Cd(SPh)_4]^{2-}$, $[Cd_4(SPh)_{10}]^{2-}$ and Cd^o in **1**} and that at ca. 725 ppm for Cd only coordinated by S^{2-} (for comparison: 706 ppm in wurtzite). An extremely broad resonance at ca. 480–880 ppm is probably due to mixed $CdS_x(SPh)_y$ environments. The peaks we observed can therefore be assigned as follows: ca. 600 ppm for $Cd(SPh)_4$, ca. 680 ppm for $CdS_2(SPh)_2$ (as Cd^i in **1**) and ca. 730 ppm for CdS_4 environments.

Contrary to the solid-state ^{113}Cd NMR spectrum of the B2 sample, the solution spectrum (Figure 8, top), only showed the byproduct signals, but no signal which could be assigned to the NPs. This was caused probably by longer relaxation times of Cd atoms in NPs. Only the "unknown" PhS group was observed in the ^{1}H NMR spectra of all reaction solutions. However, when the NPs from sample B2 were separated by precipitation with toluene and re-dispersed in [D_6]DMSO, some unresolved broad, downfield-shifted signals for PhS groups were observed beside the "unknown" PhS group (Figure 9). We suppose that the broad signals belong to PhS groups on the surface of the NPs. They were present only in samples of NPs separated by precipitation.

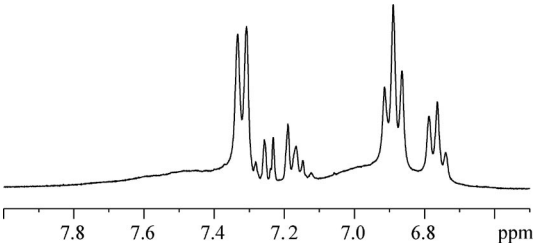

Figure 9. ^{1}H NMR spectrum of CdS NPs prepared by precipitation with toluene from sample B2 and re-dispersed in [D_6]DMSO.

In summary, we showed in the experiments of series A and B that the cluster $[Cd_{10}S_4(SPh)_{16}]^{4-}$ (**1**) is growing in DMSO solutions. At room temperature (series A), a mixture of Cd_{32} and Cd_{54} clusters was formed and no larger NPs were observed by UV/Vis absorption even after 2 months. At 80 °C (series B) cluster **1** transformed rapidly into a mixture of larger clusters and NPs. Depending on the heating period and concentration, Cd_{32} and Cd_{54} were identified by analyzing the UV/Vis spectra. The presence of larger NPs than Cd_{54} cluster was proven for heating times >4 h; the absorption edge increased to ca. 410 nm after 14 d of heating. The formed CdS NPs were separated from the reaction solutions by precipitation with toluene.

During the transformation of **1** into larger CdS NPs, we observed formation of a new PhS group in the ^{1}H and ^{13}C NMR spectra, characterized by doublet at δ = 7.31–7.32 ppm for the *ortho* protons of the PhS group. The shifts of *meta* and *para* triplets varied slightly (6.88–6.90, 6.76–6.80 ppm). In [D_7]DMF solution, also a new PhS group was formed. In the following section we will examine the origin of this "unknown" PhS group and thus characterize the byproducts which are formed during the cluster growth.

Cluster growth. There are substantial compositional differences between **1** and larger clusters or thiolate-capped CdS NPs; the S/Cd ratio increases and PhS/Cd ratio decreases with increasing size. Therefore, one or more byproducts must be formed which balance the sulfide and PhS inventory. According to Cumberland et al.,[17] $[Cd(SPh)_x(DMSO)_y]^{(2-x)}$ species could be formed.

We compared the ^{13}C NMR chemical shifts of the "unknown" PhS group with terminal and bridging PhS groups of **1**, $(Me_4N)_2[Cd(SPh)_4]$ (**2**) and $[Cd_4(SPh)_8]_\infty$ (**3**)[32] (Table 3). For bridging PhS groups the chemical shift for the *ipso* carbon atoms is ca. 140 ppm, and in terminal groups ca. 146/150 ppm. An opposite trend is observed for the *para* carbon atoms. In terminal groups they are shifted upfield by ca. 2 ppm compared to bridging groups. The same trend for *ipso* and *para* carbon atoms was observed also in [D_3]MeCN (*ipso*: 140 and 147/150 ppm, *para*: 124 and 121/122 ppm for bridging and terminal PhS group). On this basis the "unknown" PhS group in DMSO can be assigned to a terminal PhS group, assuming that it originates from a Cd–SPh species.

The B2 sample (40 mg/mL, 80 °C/16 h) showed the presence of the "unknown" PhS group in the ^{1}H NMR spectrum and broad, weak signals in the ^{113}Cd NMR spectrum at 593, 517 and 67 ppm (Figure 8, top). The resonance at δ = 593 ppm can be assigned to a $Cd(SPh)_4$ environment. The

 © 2010 Wiley-VCH Verlag GmbH & Co. KGaA, Weinheim

Table 3. Summary of the ^{13}C NMR spectroscopic data of terminal and bridging PhS groups of **1**, $(Me_4N)_2[Cd(SPh)_4]$ (**2**) and $[Cd_4(SPh)_8]_\infty$ (**3**) in $[D_6]$DMSO.

PhS group		^{13}C shifts *ipso*	*ortho*	*meta*	*para*
"unknown"		145.8	131.7–132.5	127.2–127.3	120.9
Terminal	**1**	145.4	132.5	127.1	120.6
	2	149.3	132.7	126.7	119.4
Bridging	**1**	138.7	133.6	127.1	122.9
	3	140.0	132.9	127.7	122.9

resonances at 517 and 67 ppm could indicate partial coordination of DMSO to Cd,[33] viz. $Cd(SPh)_3(DMSO)_y$ (resonance at δ = 517 ppm) and mononuclear Cd complexes with a higher proportion of DMSO (resonance at δ = 67 ppm).

In order to gain further insight, $(NMe_4)_2[Cd(SPh)_4]$ (**2**) was added in a 1:1 molar ratio to the B2 sample. Shifts in the ^{113}Cd NMR spectra changed drastically. Only one broad signal at δ = 535 ppm (Figure 8, bottom) was obtained after addition of **2** (δ = ^{113}Cd of **2** is 602 ppm). Furthermore, only one PhS group was observed in the NMR spectra after addition of **2**, the *meta* and *para* protons of which shifted slightly and which had character of a terminal group. The presence of one set of PhS resonances is probably due to fast PhS exchange between the byproduct and **2**, which is in line with our expectation.

In an attempt to crystallize some $[Cd(SPh)_x(DMSO)_y]^{(2-x)}$ species from the DMSO reaction solutions of **1** by addition of other solvents (see Exp. Sect.), we obtained crystals of the known compound $[Cd_4(SPh)_8]_\infty$ (**3**) [32] and of $(NMe_4)_2[Cd_8S(SPh)_{16}]$ (**4**). A single-crystal X-ray structure determination showed that the cluster anion of **4** has essentially the same structure as that in $(MV)[Cd_8S(SPh)_{16}]$[34] (MV = methyl viologen dication), $(NEt_4)_2[Cd_8S(SePh)_{16}]$[14] and $[Cd_8S(SePh)_{12}Cl_4]^{2-}$.[35]

In order to examine whether **3** and **4** were present in the reaction solutions directly after the heat treatment, we compared the NMR spectra of **3** and **4** with those of reaction solutions. Cluster **4** was characterized previously in DMF solution by ^{113}Cd NMR spectroscopy.[14] The integrity of the complex in solution was confirmed. The Cd^i and Cd^o resonances of **4** were at 625 and 584 ppm, respectively.[14] These values are distinctly upfield shifted compared to the Cd^i and Cd^o resonances of **1** (682.5 and 598 ppm). The shifts are different to those obtained for the B2 sample (593, 517 and 67 ppm), which suggests that **4** is not present in DMSO reaction solutions after the thermal treatment. However, as pointed out in the Introduction, clusters of different sizes are in equilibrium in solution, and **4** may be formed as the least soluble species after the change of solvent conditions.

The same applies for cluster **3**. It was previously proposed that the 3D network of Cd_4 clusters present in crystalline **3** is broken in DMF solution and aggregates of Cd_4 clusters are formed.[33] The aggregates are larger at lower temperature and disintegrate due to solvent coordination with increasing temperature. We observed a similar behavior in DMSO solution of **3**, but the temperature dependence was different. At room temperature, there was one ^{113}Cd NMR resonance at δ = 591 ppm, which was assigned to an average $Cd(SPh)_4$ environment. The ^{13}C NMR spectrum revealed one bridging PhS group. No sharp signals were observed in the ^{113}Cd NMR spectrum at 353 K. It can be concluded, that aggregates of Cd_4 clusters are present in the DMSO solution of **3** at room temperature, similarly to DMF solution at lower temperatures.[33] This shows that such aggregates of Cd_4 clusters are not present directly in the DMSO solutions. They are formed only upon addition of other solvents.

The UV/Vis spectra of CdS NPs precipitated by addition of toluene to samples B1–B4 showed a substantial decrease of absorption in the range <325 nm compared with the reaction solutions (for sample B1 see Figure 10). This can be explained by byproduct(s) with absorption <325 nm which are not or only partially precipitated from the reaction solutions. The UV/Vis spectra of DMSO solutions of $(NMe_4)_2[Cd(SPh)_4]$ (**2**) and $[Cd_4(SPh)_8]_\infty$ (**3**) (Figure 10) are similar, with absorption maxima at 279 or 272 nm, respectively. In order to find evidence whether **2**, possibly **3**, or related species are present in the DMSO solution, we calculated the spectrum of the reaction solution B1 by superposition of the spectra of re-dispersed NPs precipitated from the B1 solution and **2** in DMSO (calculation 1 in Figure 11) or both **2** and **3** in DMSO (calculation 2 in Figure 11). The value $\Sigma|(A_c - A_o)/(A_c + A_o)|$ was minimized in the range 265–400 nm in the calculations. Calculation 2 led to a better fit with the following composition for the 3.3×10^{-6} M B1 reaction solution: 5.6×10^{-6} M of **2**, 5.3×10^{-6} M of **3** and 0.0048 mg/mL of B1 NPs. Calculation 1 led to following composition: 1.2×10^{-5} M of **2** and 0.0046 mg/mL of B1 NPs. The calculated NPs yield was in good agreement with the yield determined in the previous section.

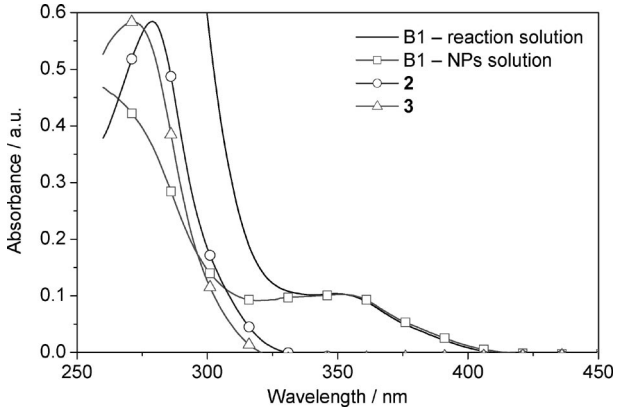

Figure 10. UV/Vis spectra of B1 reaction solution (0.028 mg/mL), re-dispersed NPs precipitated from B1 (0.013 mg/mL), $(NMe_4)_2[Cd(SPh)_4]$ (**2**) (0.009 mg/mL) and $[Cd_4(SPh)_8]_\infty$ (**3**) (0.013 mg/mL), in DMSO.

In order to draw conclusions about the nature of the byproduct and its UV/Vis similarity with **2** and **3** in DMSO solutions, the following has to be considered. First, solutions for UV spectroscopy are much diluted compared to

 © 2010 Wiley-VCH Verlag GmbH & Co. KGaA, Weinheim

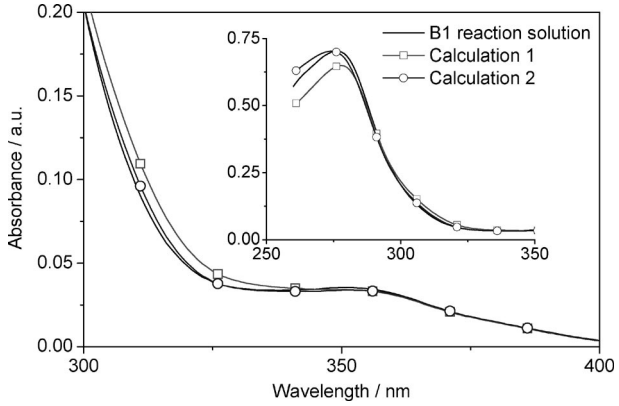

Figure 11. Calculation of the UV/Vis spectrum of the B1 reaction solution (0.011 mg/mL) using spectra of re-dispersed NPs precipitated from the B1 solution and **2** in DMSO (calculation 1) and both **2** and **3** in DMSO (calculation 2).

solutions investigated by NMR spectroscopy. This can lead to formation of other species, especially with lower nuclearities. Second, the UV/Vis behavior of very small Cd thiolate clusters is opposite to CdS NPs and exhibits blue shift with increasing complex size.[36] This explains the blue shift of **3** relative to **2** in DMSO. It also would mean that at least a part of **3** is present in the form of Cd_4 clusters in much diluted DMSO solutions of **3**, similar to the NMR investigations. Since calculation 2 led to better fit, it can be assumed that not only mononuclear Cd species are present in the reaction solutions, but also larger Cd_4 clusters. On the other hand, the absorption of mononuclear Cd species can be influenced by solvent coordination; thus, the absorption maxima of $[Cd(SPh)_x(DMSO)_y]^{(2-x)}$ species can be shifted compared with **2**. From these data the precise composition of species present in diluted DMSO reaction solutions cannot be elucidated. Nevertheless, the relatively good fit of the spectrum of the B1 reaction solution by calculation 1 allows the conclusion that the byproduct consists of some mononuclear species similar to **2**.

We thus proved in this section that the byproduct of the formation of CdS NPs from $[Cd_{10}S_4(SPh)_{16}]^{4-}$ (**1**) in DMSO solutions is a mononuclear compound with a likely composition of $[Cd(SPh)_x(DMSO)_y]^{(2-x)}$ ($x \approx 3$). This supports the prediction of Cumberland et al. about the fragmentation of **1** which was supposed to start by cleavage of its apical Cd° positions and formation of $[Cd°(SPh)_3]^-$ species.[17]

The main evidence leading to this conclusion can be summarized as follows:

1. The "unknown" PhS group observed in NMR spectra of reaction solutions is terminal, i.e. is bonded to only one Cd atom.

2. Addition of $(NMe_4)_2[Cd(SPh)_4]$ (**2**) to a reaction solution leads to only one PhS group with terminal character, which is similar to the byproduct and **2**. The shift in ^{113}Cd NMR resonance can be attributed to partial coordination of DMSO to Cd before and after addition of **2**.

3. Small clusters, viz. $[Cd_4(SPh)_8]_\infty$ (**3**) and $[Cd_8S(SPh)_{16}]^{2-}$ (**4**), were crystallized from the reaction solution, although they are not present in the reaction solutions as such.

4. Differences in the UV/Vis spectra of reaction solutions and the NPs precipitated from these solutions revealed that the byproduct has UV/Vis characteristics similar to that of **2**.

Conclusions

We have shown that the cluster $[Cd_{10}S_4(SPh)_{16}]^{4-}$ (**1**) grows in DMSO solutions. At room temperature, a mixture of Cd_{32} and Cd_{54} clusters is formed, while larger clusters and/or CdS nanoparticles are also present at 80 °C. NPs were precipitated by addition of toluene, MeOH, EtOH or acetone to the reaction solutions. Solid-state NMR confirmed the presence of PhS^- and Me_4N^+ on their surface. Cumberland et al. proposed a growth mechanism for $Li_4[Cd_{10}Se_4(SPh)_{16}]$ heated in hexadecylamine (HDA).[17] This mechanism is based on the fragmentation of the Cd_{10} cluster and loss of apical $[Cd(SePh)_3]^-$ species upon which the residual smaller Cd_xSe_y species aggregate and form larger clusters or NPs. Our findings support this mechanism. We could characterize the byproduct which formed during the transformation and found strong evidence that it is a mononuclear species with a composition $[Cd(SPh)_x(DMSO)_y]^{(2-x)}$ ($x \approx 3$).

We suppose that cluster **1** behaves similarly in other coordinating solvents. We observed growth of **1** also in DMF and acetonitrile; however it was slower in DMF and substantially slower in acetonitrile. Similar rearrangement processes must be expected for larger CdS clusters in coordinating solvents (*e.g.*, Cd_{17} clusters which reversibly change on dissolution in DMF[9]).

Experimental Section

General (Syntheses): Standard Schlenk techniques were employed for all syntheses using a double-manifold vacuum line with high-purity dry argon. Oxygen was removed from solvents using Schlenk and cannula techniques, and sparging of argon. $Cd(NO_3)_2$, PhSH, Et_3N and Me_4NCl were purchased from Aldrich and used as received. Dimethyl sulfoxide (DMSO) was distilled, dried and deoxygenated by standard techniques.

$(NMe_4)_4[Cd_{10}S_4(SPh)_{16}]$ (**1**) was synthesized as described in ref.[8] and recrystallized from boiling acetonitrile. A new polymorph of **1** (**1a**) was obtained by addition of three or seven equivalents of toluene to a 40 mg/mL (10 mg/mL) solution of **1** in DMSO after 1 d at room temperature.

Samples B1–B4 were prepared by dissolution of **1** in DMSO at room temperature followed by 30 min warming-up phase and 16 or 72 h heating phase at 80 °C. Details are summarized in Table 1.

$(NMe_4)_2[Cd(SPh)_4]$ (**2**) was prepared as described in ref.[8]. The crystals of a new polymorph of **2** (**2a**) were obtained by cooling the reaction solution to –20 °C instead of recrystallization from *i*PrOH.[37] When the crystals of **2a** were separated from the reaction mixture, and MeOH was added to the solution, monoclinic crystals of the known polymorph of **2**[37] were obtained after cooling to

 © 2010 Wiley-VCH Verlag GmbH & Co. KGaA, Weinheim

–20 °C. The molecular structure of **2a** is very similar to the known polymorph.

$[Cd_4(SPh)_8]_\infty$ (**3**)[32] was obtained by two methods: (a) addition of 10 volume equivalents of MeOH to B1 (10 mg/mL of **1** in DMSO heated at 80 °C for 16 h), followed by addition of 5 equiv. of H_2O. Centrifugation after two weeks resulted in separation of a pale yellow precipitate and a clear colorless solution. The solution was left undisturbed at room temperature for one week. This resulted in the formation of small crystals of **3**. (b) Addition of 17 equiv. of methanol to B1, followed by centrifugation after 2 weeks resulted in separation of a pale yellow precipitate and a clear colorless solution. Then 3 equiv. of water were added to the solution. This resulted in the formation of small crystals of **3** after one week. Powder XRD confirmed the presence of **3** as the only crystalline phase in both cases (Figure S4).

$(NMe_4)_2[Cd_8S(SPh)_{16}]$ (**4**) was obtained from reaction solution B1 (10 mg/mL of **1** in DMSO heated at 80 °C for 16 h) by addition of 8 volume equivalents of MeOH and 6 equiv. of H_2O, centrifugation after few days and addition of 3 equiv. of *i*PrOH. Crystals were formed after 7 d of standing at room temperature; yield 18% based on **1**.

General (Physical Measurements): Solution UV/Vis absorption spectra were recorded on a Perkin–Elmer Lambda 35 UV/Vis spectrophotometer in 1 cm quartz cuvettes against air. Spectra of the pure solvents were subtracted. Solid-state spectra of the micron-sized powders were measured in mineral oil dispersions between quartz plates with a Labsphere integrating sphere.

Dynamic light-scattering (DLS) experiments were performed with an ALV/CGS-3 Compact Goniometer system equipped with an ALV/LSE-5003 Multiple τ Digital Correlator (ALV-GmbH, Germany) at a scattering angle of 90° and a 632.8 nm JDSU laser 1145P. All measurements were carried out at 25 ± 0.1 °C in glass containers. Measured intensity correlation functions were regularized fitted by $g_2(t)$ function with radius distribution limits 0.5 and 2500 nm. Mass weight linear distribution functions were presented.

Powder X-ray diffraction measurements were performed on a Philips X'Pert Pro diffractometer system [Cu K_α radiation (λ = 1.542 Å) equipped with an X'Celerator multi-channel detector, Bragg–Brentano geometry]. The samples were placed on a single-crystal Si wafer sample holder and measured with a rate of 3°/min.

Small-angle X-ray scattering (SAXS) measurements were performed with Cu-K_α radiation from a rotating anode generator (Nanostar, Bruker AXS) equipped with a pinhole camera and an area detector (VANTEC 2000). The SAXS intensity patterns were corrected for background scattering and then radially averaged to obtain the function $I(q)$, where $q = (4\pi/\lambda)\sin\theta$ is the scattering vector, 2θ the angle between incident and diffracted beam, and λ = 0.1542 nm the X-ray wavelength. The scattering intensities $I(q)$ were fitted with asymmetric Gaussian and Lorentzian functions for the samples with a concentration of 10 mg/L (B1 and B3) and 40 mg/L (B2 and B4), respectively (Figure S5). The maximum and the half-width from the fits in reciprocal space were then converted into NP distances and distribution widths in real space.

Solution NMR spectra were recorded on a Bruker DPX 300 (^{1}H at 300.13 MHz, ^{13}C at 75.47 MHz, ^{113}Cd at 66.61 MHz) equipped with a 5-mm inverse-broadband probe head with a *z*-gradient unit. 2D experiments were measured with Bruker standard pulse sequences [COSY (Correlated Spectroscopy), HSQC (Heteronuclear Single Quantum Correlation), HMBC (Heteronuclear Multiple-Bond Correlation), ^{1}H-^{113}Cd HMBC]. Cluster **1** in [D_3]acetonitrile, [D_6]DMSO and [D_7]DMF solutions was measured at concentration 10 mg/mL. Cluster **3** in [D_6]DMSO was measured at concentration 100 mg/mL. Shifts for solution ^{113}Cd NMR were referenced against 1 M $Cd(NO_3)_2$ (aq.) (δ = 0). For comparison, literature data were re-calculated to 1 M $Cd(NO_3)_2$ (aq.) as reference. 0.1 M $Cd(NO_3)_2$ (aq.) resonates at δ = 17 ppm, while the chemical shift difference is 65 ppm for $Cd(NO_3)_2$ (aq.) from 4 M to infinite dilution.[38] NMR solvents were purchased from euriso-top in high purity grade.

Solid-state NMR spectra were recorded on a Bruker Avance 300 (^{13}C at 75.47 MHz, ^{113}Cd at 66.54 MHz) equipped with a 4 mm broadband MAS probe head. ^{13}C NMR spectra were recorded with ramped CP/MAS (Cross Polarization and Magic Angle Spinning) and ^{113}Cd NMR spectra with HPDEC (High-power Decoupling).

Table 4. Crystallographic data for $(NMe_4)_4[Cd_{10}S_4(SPh)_{16}]$ (**1a**), $(NMe_4)_2[Cd(SPh)_4]$ (**2a**) and $(NMe_4)_2[Cd_8S(SPh)_{16}]$ (**4**).

	1a	**2a**	**4**
Formula	$C_{112}H_{128}Cd_{10}N_4S_{21.5}$	$C_{32}H_{44}Cd_1N_2S_4$	$C_{104}H_{110}Cd_8N_2O_3S_{17}$
Formula weight	3343.47	697.33	2880.16
Crystal size [mm]	$0.28 \times 0.20 \times 0.15$	$0.05 \times 0.05 \times 0.03$	$0.25 \times 0.03 \times 0.03$
Crystal system	orthorhombic	tetragonal	monoclinic
Space group	*Aba*2	$P4_32_12$	$P2_1/n$
a [pm]	2799.8(6)	1032.46(6)	1837.2(5)
b [pm]	2931.7(6)		2529.7(7)
c [pm]	1693.3(3)	3273.1(4)	2517.4(7)
β [°]			102.861(4)
V [pm^3] $\times 10^6$	13899(5)	3489.0(5)	11406(5)
Z	4	4	4
$\rho_{calcd.}$ [g cm^{-3}]	1.598	1.328	1.677
μ [mm^{-1}] (Mo-K_α)	1.862	0.888	1.820
θ_{max} [°]	28.33	25.00	25.00
Refections measured	64719	19452	40725
Unique reflections	17078	3078	19602
Reflections $I > 2\sigma(I)$	13201	1865	10818
Parameters	708	303	1293
R_1 [$I > 2\sigma(I)$]	0.048	0.046	0.052
wR_2 [$I > 2\sigma(I)$]	0.117	0.059	0.105
GOF for I^2	1.147	1.005	0.961
Min./max. [e Å^{-3}]	1.25/–1.25	0.28/–0.31	1.60/–1.12

 © 2010 Wiley-VCH Verlag GmbH & Co. KGaA, Weinheim

The rotor spinning speed was 6 kHz. Shifts were referenced against 1 M $Cd(NO_3)_2$ (aq.) ($\delta = 0$).

X-ray Structure Analyses: Crystals suitable for single-crystal X-ray diffraction were taken directly from the reaction solutions, selected in perfluoropolyether oil, mounted on a Bruker AXS KAPPA APEX II diffractometer with an APEX II CCD area detector and measured in a nitrogen stream at 100 K (**2a** was measured at 298 K). Graphite-monochromated Mo-K_α radiation (λ = 71.073 pm) was used for all measurements. The data collection covered at least a hemisphere of the reciprocal space using 0.3° ω-scan frames. The crystal-to-detector distance was 5 cm. The data were corrected for polarization and Lorentz effects, and corrections for absorption and $\lambda/2$ effects were applied.

The structures were solved with direct methods and were then refined by the full-matrix least-squares method based on $F2$ using the program package SHELXTL (Bruker AXS Inc.). All non-hydrogen atoms were refined with anisotropic displacement parameters. Hydrogen atoms were placed on calculated positions. Some of the phenyl rings were disordered over two positions. In this case, their carbon atoms were constrained to form a regular hexagon. Important parameters for all structures are summarized in Table 4.

CCDC-762159 (for **1a**), -762160 (for **2a**) and -762161 (for **4**) contain the supplementary crystallographic data for this paper. These data can be obtained free of charge from The Cambridge Crystallographic Data Center via www.ccdc.cam.ac.uk/data_request/cif.

Supporting Information (see also the footnote on the first page of this article): Supporting information contains additional data on the ^{1}H NMR spectra of **1** in different solvents, additional UV/Vis spectra, X-ray powder diffractogram of **3**, and measured and fitted SAXS curves.

Acknowledgments

The authors thank the Austrian Science Funds (FWF) for financial support (project P19199), Dipl.-Ing. Berthold Stöger and Dipl.-Ing. Gerhard Wieser, Vienna University of Technology, for powder XRD analyses, and Prof. Kurt Mereiter, Vienna University of Technology, for help with single-crystal X-ray analyses.

[1] H. Weller, *Adv. Mater.* **1993**, *5*, 88–95.
[2] a) A. P. Alivisatos, *J. Phys. Chem.* **1996**, *100*, 13226–13239; b) A. P. Alivisatos, *Science* **1996**, *271*, 933–937.
[3] a) L. E. Brus, *J. Chem. Phys.* **1984**, *80*, 4403–4409; b) R. Rossetti, J. L. Ellison, J. M. Gibson, L. E. Brus, *J. Phys. Chem.* **1984**, *80*, 4464–4469 .
[4] N. Zheng, X. Bu, H. Lu, Q. Zhang, P. Feng, *J. Am. Chem. Soc.* **2005**, *127*, 11963–11965.
[5] T. Vossmeyer, G. Reck, L. Katsikas, E. T. K. Haupt, B. Schulz, H. Weller, *Science* **1995**, *267*, 1476–1479.
[6] T. Vossmeyer, G. Reck, B. Schulz, L. Katsikas, H. Weller, *J. Am. Chem. Soc.* **1995**, *117*, 12881–12882.
[7] M. Bendova, M. Puchberger, U. Schubert, *Chem. Eur. J.*, submitted.
[8] I. G. Dance, A. Choy, M. L. Scudder, *J. Am. Chem. Soc.* **1984**, *106*, 6285–6295.
[9] G. S. H. Lee, D. C. Craig, I. Ma, M. L. Scudder, T. D. Bailey, I. G. Dance, *J. Am. Chem. Soc.* **1988**, *110*, 4863–4864.
[10] N. Herron, J. C. Calabrese, W. E. Farneth, Y. Wang, *Science* **1993**, *259*, 1426–1428.
[11] N. Zheng, X. Bu, J. Lauda, P. Feng, *Chem. Mater.* **2006**, *18*, 4307–4311.
[12] N. Zheng, H. Lu, X. Bu, P. Feng, *J. Am. Chem. Soc.* **2006**, *128*, 4528–4529.
[13] a) I. Dance, K. Fisher, *Prog. Inorg. Chem.* **1994**, *41*, 637–803; b) I. Dance, K. Fisher, G. Lee, *Metallothioneins* **1992**, 284–345; c) I. Dance, G. Lee, *Spec. Publ.- R. Soc. Chem.* **1993**, *131*, 87–94.
[14] G. S. H. Lee, K. J. Fisher, D. C. Craig, M. L. Scudder, I. G. Dance, *J. Am. Chem. Soc.* **1990**, *112*, 6435–6437.
[15] T. Lover, W. Henderson, G. A. Bowmaker, J. M. Seakins, R. P. Cooney, *Inorg. Chem.* **1997**, *36*, 3711–3723.
[16] I. G. Dance, *Aust. J. Chem.* **1985**, *38*, 1745–1755.
[17] S. L. Cumberland, K. M. Hanif, A. Javier, G. A. Khitrov, G. F. Strouse, S. M. Woessner, C. S. Yun, *Chem. Mater.* **2002**, *14*, 1576–1584.
[18] G. Berrettini Mia, G. Braun, G. Hu Jerry, F. Strouse Geoffrey, *J. Am. Chem. Soc.* **2004**, *126*, 7063–7070.
[19] M. W. DeGroot, H. Rosner, J. F. Corrigan, *Chem. Eur. J.* **2006**, *12*, 1547–1554.
[20] D. D. Lovingood, R. E. Oyler, G. F. Strouse, *J. Am. Chem. Soc.* **2008**, *130*, 17004–17011.
[21] Z. Li, W. Cai, J. Sui, *Nanotechnology* **2008**, *19*, 1–7.
[22] C. Tuinenga, J. Jasinski, T. Iwamoto, V. Chikan, *ACS Nano* **2008**, *2*, 1411–1421.
[23] M. W. DeGroot, N. J. Taylor, J. F. Corrigan, *Inorg. Chem.* **2005**, *44*, 5447–5458.
[24] T. T. Türk, U. Resch, M. A. Fox, A. Vogler, *J. Phys. Chem.* **1992**, *96*, 3818–3822.
[25] I. G. Dance, J. K. Saunders, *Inorg. Chim. Acta* **1985**, *96*, L71–L73.
[26] K. S. Hagen, D. W. Stephan, R. H. Holm, *Inorg. Chem.* **1982**, *21*, 3928–3936.
[27] T. Vossmeyer, L. Katsikas, M. Giersig, I. G. Popovic, K. Diesner, A. Chemseddine, A. Eychmueller, H. Weller, *J. Phys. Chem.* **1994**, *98*, 7665–7673.
[28] H. Döllefeld, H. Weller, A. Eychmüller, *Nano Lett.* **2001**, *1*, 267–269.
[29] O. Alvarez-Fregoso, J. G. Mendoza-Alvarez, O. Zelaya-Angel, *J. Appl. Phys.* **1997**, *82*, 708–711.
[30] W. W. Yu, X. Peng, *Angew. Chem. Int. Ed.* **2002**, *41*, 2368–2371.
[31] N. Herron, Y. Wang, H. Eckert, *J. Am. Chem. Soc.* **1990**, *112*, 1322–1326.
[32] D. Craig, I. Dance, R. Garbutt, *Angew. Chem.* **1986**, *98*, 178–179.
[33] I. G. Dance, R. G. Garbutt, T. D. Bailey, *Inorg. Chem.* **1990**, *29*, 603–608.
[34] K.-L. Tang, X.-L. Jin, S.-J. Jia, Y.-Q. Tang, *Jiegou Huaxue* **1995**, *14*, 399–404.
[35] Q. Zhang, T. Wu, X. Bu, T. Tran, P. Feng, *Chem. Mater.* **2008**, *20*, 4170–4172.
[36] H.-J. Liu, J. T. Hupp, M. A. Ratner, *J. Phys. Chem.* **1996**, *100*, 12204–12213.
[37] N. Ueyama, T. Sugawara, K. Sasaki, A. Nakamura, S. Yamashita, Y. Wakatsuki, H. Yamazaki, N. Yasuoka, *Inorg. Chem.* **1988**, *27*, 741–747.
[38] R. J. Kostelnik, A. A. Bothner-By, *J. Magn. Reson.* **1974**, *14*, 141–151.

Received: January 27, 2010
Published Online: April 14, 2010

 © 2010 Wiley-VCH Verlag GmbH & Co. KGaA, Weinheim